AD-A278 387

DOCUMENTATION PAGE

Form Approved
OMB No. 0704-0188

information is estimated to average 1 hour per response, including the time for reviewing instructions, searching existing data sources, and completing and reviewing the collection of information. Send comments regarding this burden estimate or any other aspect of this is for reducing this burden, to Washington Headquarters Services, Directorate for information Operations and Reports, 1215 Jefferson 02-4102, and to the Office of Management and Budget, Paperwork Reduction Project (0704-0188), Washington, DC 20503

nk)	2. REPORT DATE	3. REPORT TYPE AND DATES COVERED
	OCT-1993	ANNUAL - 15 Sep 92 to 14 Sep 93

4. TITLE AND SUBTITLE

FUNDAMENTAL STUDIES IN CRACK INITIATION

5. FUNDING NUMBERS

F4962.0
92-J-0493
2302/DS
(2)

6. AUTHOR(S)

John Botsis

7. PERFORMING ORGANIZATION NAME(S) AND ADDRESS(ES)

Department of Civil Engineering,
Mechanics and Metallurgy (mc 246)
University of Illinois, Chicago
842 W Taylor Str. Chicago IL 60607

8. PERFORMING ORGANIZATION REPORT NUMBER

AFOSR-TR- 94 0227

9. SPONSORING/MONITORING AGENCY NAME(S) AND ADDRESS(ES)

Air Force Office of Scientific Research
Aerospace and Engineering Sciences
Building 410, Bolling AFB
Washington D.C. 20332

N/A

10. SPONSORING/MONITORING AGENCY REPORT NUMBER

F49620-
92-J-0493

11. SUPPLEMENTARY NOTES

N/A

DTIC
ELECTE
APR 20 1994
S F D

12a. DISTRIBUTION/AVAILABILITY STATEMENT

Approved for public release;
Distribution unlimited

12b. DISTRIBUTION CODE

N/A

13. ABSTRACT *(Maximum 200 words)*

Mechanistic investigations of damage evolution before crack initiation in an amorphous polymer show that damage consists of a core of highly dense crazing and a peripheral less dense zone of crazing. Damage characterization is carried out at consecutive configurations of the damage zone. Analysis of the kinematics of damage at different times involves comparisons of the inertia moments of damage distributions. The results indicate that damage evolution between consecutive configurations can be approximated by a linear transformation of the space variables. Thus, the process of damage growth can be described by translation and deformation of the damage zone. The growth can be described by translation and deformation of the damage zone. The growth rates of the damage zone movements decrease until crack initiation. In all cases, the average densities exhibit a damping type behavior with the number of cycles. The crack initiates within a core zone immediately ahead of the stress concentrator. The experimental results suggest that damage density within the core zone is independent of the loading conditions considered herein. This value is approximately equal to the damage density around the crack tip during slow crack propagation. The crack length at initiation is found to increase exponentially with the stress level. A simple decaying exponential relationship relates the crack initiation times and the applied stress level. This result is consistent with the fracture models based on absolute reaction theories.

14. SUBJECT TERMS	15. NUMBER OF PAGES
Fatigue, Damage Evolution, Translation-Expansion Critical Damage	37
	16. PRICE CODE

17. SECURITY CLASSIFICATION OF REPORT	18. SECURITY CLASSIFICATION OF THIS PAGE	19 SECURITY CLASSIFICATION OF ABSTRACT	20. LIMITATION OF ABSTRACT
UNCLASSIFIED	UNCLASSIFIED	UNCLASSIFIED	

AFOSR-TR- 94 0227

Approved for public release;
distribution unlimited.

FUNDAMENTAL STUDIES IN CRACK INITIATION

Yearly Report
October 1993

Prepared by

John Botsis
Associate Professor of
Mechanics and Materials

Department of Civil Engineering,
Mechanics & Metallurgy
2095 ERF, 842 W. Taylor Str.
University of Illinois at Chicago
Chicago, IL 60607

for

Air force Office for Scientific Research
Grand No. 92-J-0493

94-11922

DTIC QUALITY INSPECTED 3

1 94 4 19 038

TABLE OF CONTENTS

Accesion For

NTIS CRA&I

DTIC TAB

Unannounced

Justification

By

Distribution /

Availability

Dist | Avail and/or Special

A-1

LIST OF TABLES

LIST OF FIGURES

Objectives

This project was set to, (a) investigate the kinematics of damage before crack initiation, (b) formulate kinetic equations for damage growth, and (c) derive criteria for crack initiation in an amorphous material. ***From the research so far, the following important results have emerged:***

1. Damage accompanies the process of crack initiation. The damage zone consist of a core zone with highly localized damage and a peripheral less dense damage zone.

2. While the pattern of the peripheral zone is depended upon the loading history, the density in the core zone is independent of the loading history.

3. The kinematics of damage before crack initiation can be described by an affine transformation of the space variables. Accordingly, damage evolution can be described by the translation, isotropic expansion and homogeneous distortion of the damage zone.

4. The time to crack initiation is related to the stress level with an exponentially decaying relationship. The results agree with fracture models based on kinetic theories for submicoscopic flaw nucleation.

The results of the present studies and those reported in [17,18] indicate certain similarities between the characteristics of damage before crack initiation and during slow crack growth. These are, (a) damage evolution can be described by a linear transformation, (b) the densities of damage within a core zone at crack initiation and during slow crack growth are of the same level.

Relevant publications

The work so far has resulted in two papers that have been submitted for publication:

1. J. Botsis and C. Huang, 'Experimental and Analytical Studies in Crack Initiation under Fatigue: Part I - Experimental', *International Journal of Fracture*, Submitted, August, 1993.

2. J. Botsis and C. Huang, 'Experimental and Analytical Studies in Crack Initiation under Fatigue: Part II - Analysis', *International Journal of Fracture*, Submitted, August, 1993.

Future Work

A. Energy calculations due to damage

B. Kinetic equations for damage growth

C. Criteria fro crack initiation

The results obtained so far are given in the subsequent pages.

Summary

Mechanistic investigations of damage evolution before crack initiation in an amorphous polymer show that damage consists of a core of highly dense crazing and a peripheral less dense zone of crazing. Damage characterization is carried out at consecutive configurations of the damage zone. Analysis of the kinematics of damage at different times involves comparisons of the inertia moments of damage distributions. The results indicate that damage evolution between consecutive configurations can be approximated by a linear transformation of the space variables. Thus, the process of damage growth can be described by translation and deformation of the damage zone. The growth rates of the damage zone movements decrease until crack initiation. In all cases, the average densities exhibit a damping type behavior with the number of cycles. The crack initiates within a core zone immediately ahead of the stress concentrator. The experimental results suggest that damage density within the core zone is independent of the loading conditions considered herein. This value is approximately equal to the damage density around the crack tip during slow crack propagation. The crack length at initiation is found to increase exponentially with the stress level. A simple decaying exponential relationship relates the crack initiation times and the applied stress level. This result is consistent with the fracture models based on absolute reaction theories.

1. Introduction and Background

Prediction of life time of a structural component subjected to fatigue or creep loads assumes a position of prominence in engineering design. It becomes even more important when considering the continuous increase in complexity of engineering structures and the large costs resulting from premature failures. Thus, characterization of the mechanisms leading to crack initiation and growth is an issue of central importance to engineers and material scientists.

Contemporary approaches to life time prediction consider a fracture process in three phases: crack initiation, slow crack growth, and fast fracture. The latter phase is very short in duration and thus, the time of crack initiation and that of slow crack growth account for the useful time of a structure.

Significant efforts have been devoted to studying slow crack propagation in various materials. This is demonstrated by the vast amount of experimental data and several models that have been proposed to describe crack growth with the stress intensity factor K_1, or energy release rate J_1 [1, 2]. These analyses play an important role in life time prediction. However, experimental and theoretical studies of crack initiation have received limited attention in the literature. Moreover, fracture mechanics approaches to fatigue do not consider crack initiation [1]. Instead, the concept of crack growth threshold is employed [3, 4]. Values of fatigue threshold indicate the cyclic stress intensity factor ΔK_{th}, below which long cracks remain dormant. The corresponding ΔK_{th} is taken as a material parameter. Although the study of fatigue thresholds and near threshold behavior has highlighted the effects of load history in influencing crack growth, and has provided insight into the different mechanisms of crack closure, the threshold idea has met with limited success in engineering design. This stems

from the fact that the use of a fatigue threshold represents a conservative design criterion and from questions regarding ΔK_{th} as a material parameter [5-7].

Mechanistic investigations in various materials have shown that fatigue crack initiation and growth are preceded by various forms of damage that nucleate at heterogeneities within the material. In metals initiation is related to intense slip processes, extrusions-intrusions and persistent slip bands [8, 9]. Microcracks nucleated at inclusions or second phase particles in the case of smooth specimens have also been reported by several researchers. Observations of the same process in both notched and smooth specimens of polymers have emphasized the role of crazing in amorphous and semi - crystalline polymers [10-13]. Damage nucleation and growth, whether in the form of microcracks, voids, homogeneous transformations, crazes, etc., are processes that absorb energy, energy that otherwise would be available to drive the crack. Therefore the nature and extent of damage determine the time to crack growth and toughness of the material. Under these circumstances, use of fracture mechanics parameters may not be always justified. That is, when the restrictions of 'K-dominance' or 'J_1-dominance' are not met, K_1 and J_1 fail to correlate with the fracture process. Examples are large scale plasticity, microcrack interaction, the behavior of small cracks, etc.

Recognizing the importance of damage on crack initiation and growth, several analytical approaches have been developed to account for its effects on stress intensity factor and energy release rates (for a recent review see [14] and references therein). It is difficult, however, to assess the contributions of crack damage interactions, describe the local kinetics, and the effects of the microstructure when a large number of microdefects is present. These powerful mechanisms are the main obstacles in modeling fracture in a large class of modern engineering materials.

One way to treat fracture phenomena where dense damage accompanies crack initiation and growth is to use the ideas of self - similarity. Drawing on the success of statistical self - similarity of vortex cascade in understanding turbulence, it is proposed that the same principles can be applied to damage and fracture of engineering materials [15,16]. Indeed, experimental observations in a number of materials have shown that damage growth displays certain invariant characteristics. For example, the evolution of a normalized pore size distribution in polycrystalline steel under creep follows a pattern that is independent of time and strain level [15]. Furthermore, it has been shown that damage growth within a process zone during fatigue fracture can be described by a self - similar transformation of the space variables [17]. Modeling of such fracture processes has been made by introducing additional kinematic parameters on the basis of self - similarity [16].

Formulations of constitutive equations for damage growth and criteria for crack initiation are well recognized by now to be important problems in fracture research. Although, important progress has been made in this direction, a number of questions still remain to be properly addressed and resolved for a better understanding of fracture. In this project, inquiries into the characteristics of damage evolution before crack initiation and criteria for crack initiation are addressed. In the first phase, experimental studies on damage evolution are reported using amorphous polystyrene as a model material. To facilitate experimental observations, the site of crack initiation is located in space by inducing a 60^{o} -V notch onto the mid-span of the specimen edge. Hence, efforts are concentrated on characterizing damage dissemination, the associated kinematic parameters, and the time to crack initiation. In the second phase, the energy release rate due to damage growth is evaluated using of a semi - empirical method and experimental measurements. On the basis of the

experimental results damage growth in front of the notch tip is modeled with a first order reaction equation.

2. Experimental Procedures

2.1 Material and Specimens

Commercially available amorphous polystyrene (PS) from Transilwrap, Chicago, IL, was employed in the studies of crack initiation. The material was received in the form of sheets with dimensions of 200x250 mm. Strips of 150x22x0.20 mm were cut from these sheets with a razor blade and sandwiched between two pieces of acrylic with dimensions 150x21x6.5 mm. The specimens were squared up to 150x20x0.20 mm with the use of a fly cutter on a milling machine. The speeds of the fly cutter and the longitudinal power feed of the working table that supports the specimens were 11 rotation·sec^{-1}. and 0.23 mm·sec^{-1}, respectively. First, sections of about 0.25 mm thick were cut off the block of specimens until the edges of the specimens were on the same plane. The final few cuts were in the order of 0.01 mm so that the induced damage was minimized. The block was then flipped over and the same procedure was repeated until the desired width was achieved. The machined edges were metallographically polished to a 0.5μm finish to prevent formation of edge crazes. A double angle cutter of 60^{o} was used to notch the specimens prior to their removal from the block. Subsequently the specimens were removed from the block and washed carefully with distilled water. Note that this procedure of specimen preparation ensures identical notch tip geometries. Finally, the specimens were annealed in a temperature of 10^{o}C degrees lower than T_g (glass transition temperature) for 48 hours and then allowed to slowly cool down to room temperature. Annealing was aimed at relieving any residual stresses and healing any damage formed during the cutting procedures.

2.2 Experimental Methods

Tension - tension fatigue experiments were conducted on an Instron Testing System in laboratory environment at ambient temperature. All experiments were performed under load controlled mode with sinusoidal wave form. The evolution of damage around the notch tip was observed by means of a traveling optical microscope attached to the Instron Testing System. The fracture process was recorded using a motor driven camera that was attached to the microscope. Craze distribution was evaluated from optical micrographs of sectioned specimens (approximately 10-20μm thick) which were prepared by standard metallographic and polishing procedures. Damage density distributions were obtained by covering the micrographs of the polished sections with a mesh of rectangles. The size of a typical mesh depended upon the extent of damage around the notch tip and was about $N_1 x N_2 \approx 10x15$ (Figure 1). In all cases the dimensions of the rectangles were approximately 12x12μm. In each rectangle, the number of crazes was counted. Craze density was evaluated as number per unit area p [#/mm^2] or as $\rho = \frac{nbt}{abt}$ [mm^2/mm^3]. ρ represents the amount of area of craze mid planes per unit volume, n is the number of intersections of crazes with the vertical test line at the respective rectangle, a and b were the height and width of a rectangle, respectively, and t is the specimen thickness.

The most direct way to experimentally measure damage growth rates are by examination of sectioned samples that have been exposed to a well controlled loading history. In this way damage growth is "frozen in" at different degrees of development. Thus, to obtain damage distribution and growth rates before initiation, the experiments designed for damage evolution studies were interrupted at appropriate time intervals. Subsequently, the specimens were polished and the number of crazes in each rectangle was evaluated.

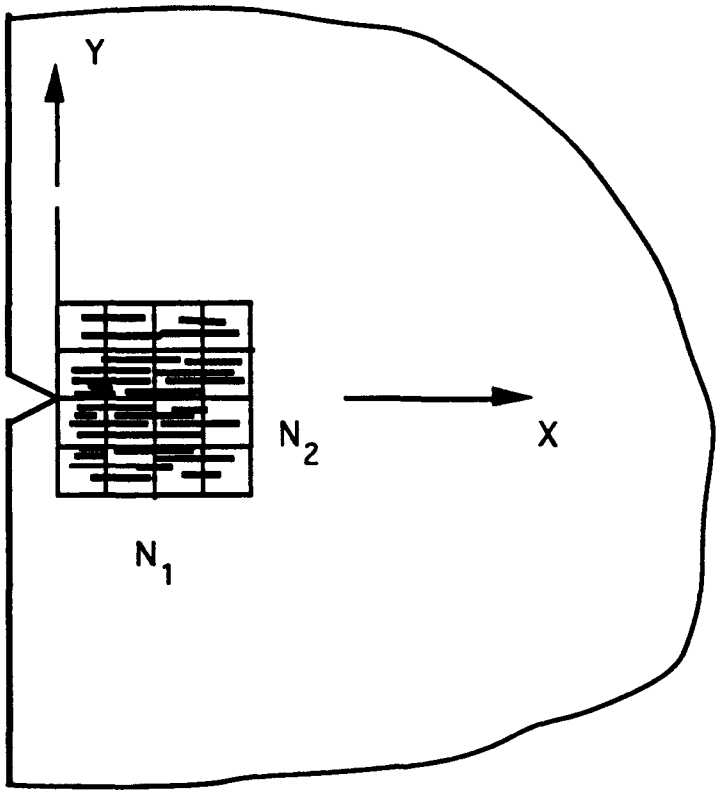

Figure 1 Schematic of a mesh of rectangles used in damage measurements.

The approach of characterizing damage described in the preceding paragraphs implies that, at a given time, damage distribution around the stress concentrator is reproducible for a certain set of loading conditions and specimen geometry. Damage accumulation, however, is a stochastic process. Accordingly, damage distribution should result from averages of a sufficiently large number of distributions observed on identical specimens. However, such an effort is experimentally difficult to carry out. Commercially available PS is a relatively 'ductile' material. This results in a large extent of crazing during crack initiation and slow crack growth [17,18]. Thus, damage within a zone in this material is amenable to a statistical treatment. To examine the reproducibility of damage distribution, two experiments were performed under the same loading conditions and specimen geometry.

The time to crack initiation was examined under the loading histories shown in Table I. Crack initiation was considered when a crack, however small, would appear at the notch tip. This event was observed with the use of a Nikon optical microscope under a magnification of x200. It has been shown that crack initiation time in PS under fatigue loads exhibits a variability of about 10% [19]. This scatter was considered small and thus, efforts were concentrated at investigating damage growth before initiation under three loading conditions, which are referred to as C1, C2, and C3. Four experiments were conducted under C1 and three under each of C2 and C3 conditions. The loads and frequency for these three sets of experiments are shown in Table I.

Due to difficulties associated with measuring an accurate crack size at initiation using an optical technique, the tests were interrupted shortly after crack initiation. Subsequently, the specimens were pulled to fracture. A crack size at initiation was assessed by examination of the fracture surfaces and its

dependence on the stress level was evaluated by performing fatigue tests under different loads.

Table I: *Loading Conditions for Crack Initiation Times and Damage Evolution Studies.*

	σ_{max} (MPa)	σ_{min} (MPa)	Frequency (sec^{-1})	Cycles to Initiation ($x10^3$)
C1:	8.00	2.75	0.33	300±10
C2:	10.50	2.75	0.33	30±2.5
C3:	14.30	2.75	0.33	4±0.5
	12.00	3.00	0.33	20±2.0
	13.00	3.00	0.33	10±1.2

3. Results and Discussion

Upon application of the load, a core zone of crazes appeared at the notch tip. While this zone increased in size, few arched crazes nucleated and propagated around the core zone. As time progressed, the crazes grew longer as well as new crazes appeared in and around the vicinity of the core. A series of optical micrographs taken during a typical experiment is shown in Figure 2. Crack initiation was defined at the instance when a crack appeared at the notch tip.

One way to investigate damage evolution is to compare the contours of equal damage density at consecutive configurations. Such pointwise comparison, however, may not be appropriate because of local fluctuations in damage density. Indeed, the contours of equal damage level at each configuration obtained from different specimens exhibit noticeable fluctuation on the scale of several micrometers (Figures 3 to 7).

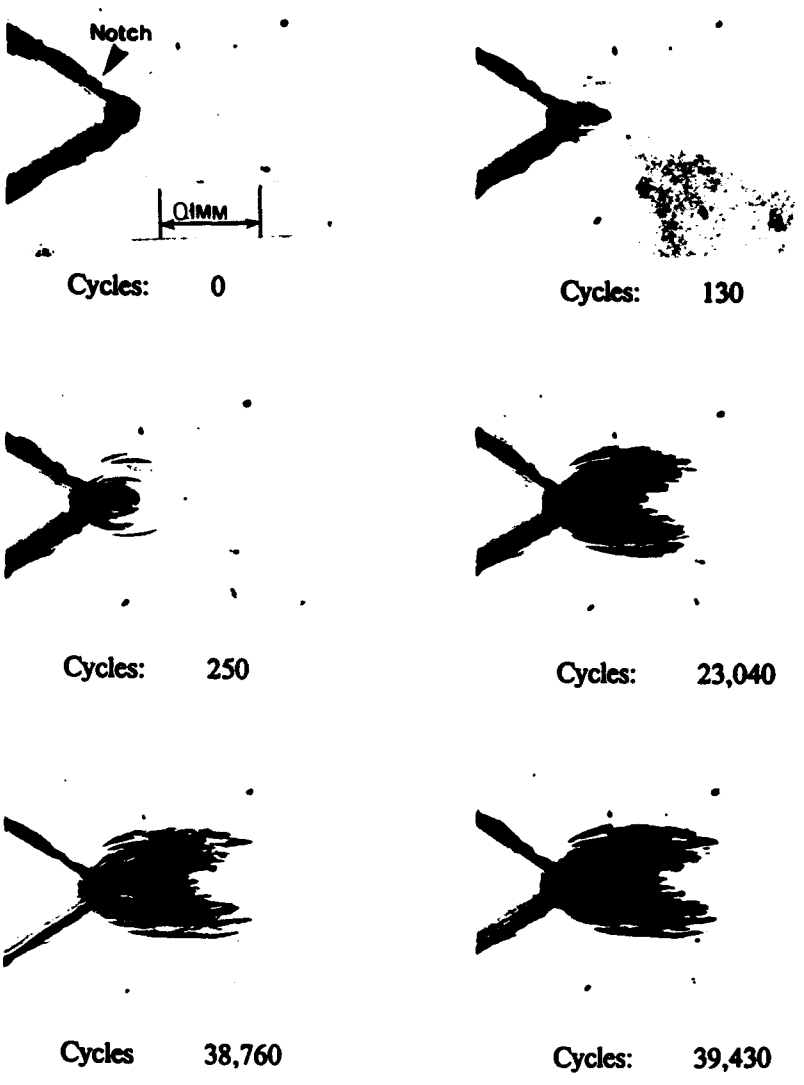

Figure 2 Series of optical micrographs showing damage growth before crack initiation.

Therefore integral parameters, such as the moments of damage distribution, were used here to evaluate the properties of damage evolution before crack initiation.

Characterization of any distribution with the use of moments should involve comparison of a sufficiently large number of moments. However, relatively high order moments may not be appropriate to compare because the experimental error built into the measurement makes them relatively inaccurate. In the present analysis, the distributions of damage were characterized by the total number of crazes within the zone I_0, the second I_{2x}, I_{2y} and fourth I_{4x}, I_{4y}, and I_{2x2y} central moments. These quantities were evaluated from the following expressions,

$$I_0 = \sum_{i=1}^{N_1} \sum_{j=1}^{N_2} p_{ij}\,, \qquad I_{mxny} = \sum_{i=1}^{N_1} \sum_{j=1}^{N_2} [x_{ij}-x_c]^m [y_{ij}-y_c]^n p_{ij} \Delta y_j \Delta x_i$$

Here $i = 1,...N_1$ and $j = 1,...N_2$ refer to the size of the mesh (see Figure 1) and m, n stand for the order of the moments and take values of, 0, 2, or 4. x_c and y_c are the coordinates of the damage zone center with reference to the notch tip and given by,

$$x_c = \sum_{i=1}^{N_1} \sum_{j=1}^{N_2} x_{ij} p_{ij}\, \Delta y_j \Delta x_i \Big/ \sum_{i=1}^{N_1} \sum_{j=1}^{N_2} p_{ij}\, \Delta y_j \Delta x_i\,, \; y_c = 0$$

y_c is zero due to symmetry of the damage zone around the y axis (Figure 3).

The contours of equal damage density ρ, pertaining to two specimens fatigued under conditions C2 (Table I) and up to the instance of crack initiation are displayed in Figure 3. Note that, the contours of damage density have been symmetrized with respect to the bisector of the V-notch because small variations

in density were observed at some points located at equal distances from the X axis. These differences were attributed to local fluctuation in damage density.

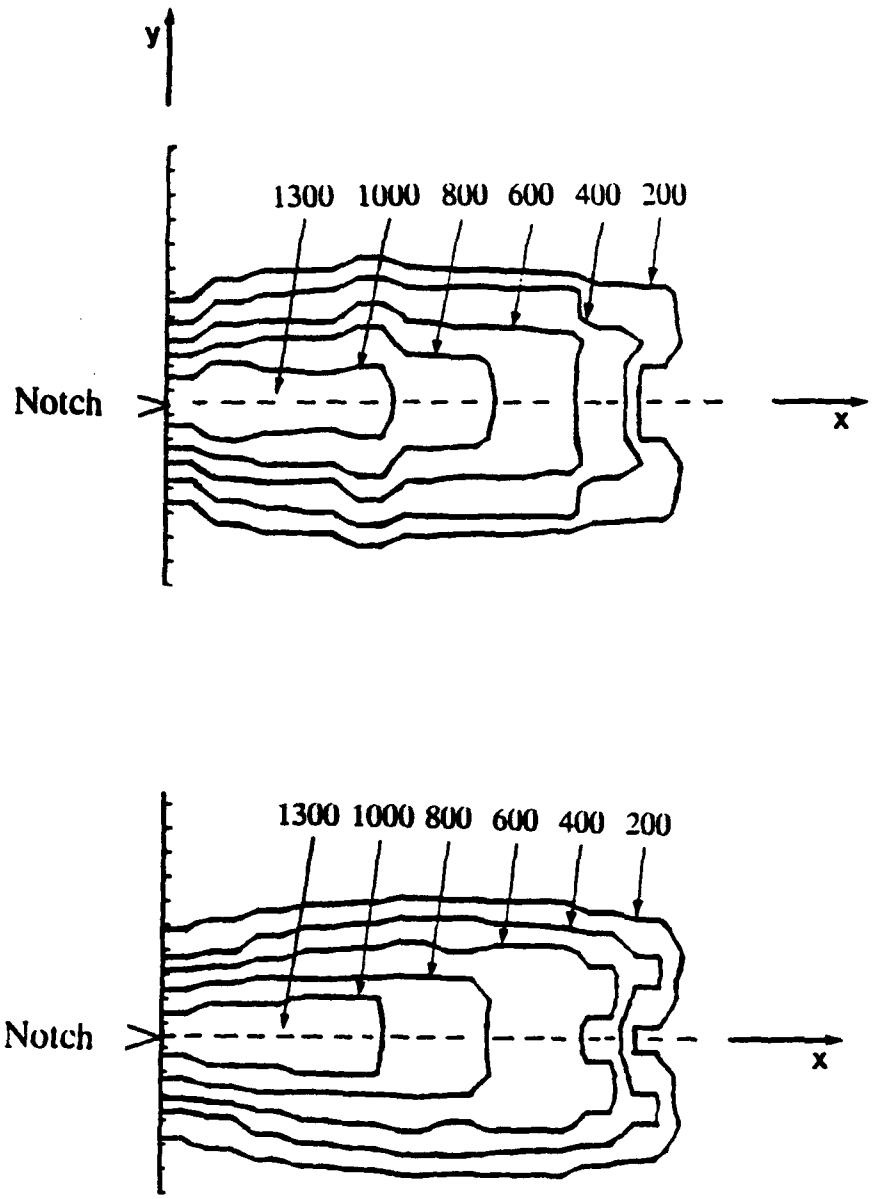

Figure 3 Contours of equal damage density ρ [mm^2/mm^3], for two specimens fatigued under the same conditions and equal times (Conditions C2).

Thus, the density at these locations was substituted with the arithmetic mean of the respective density values. For the sake of visual clarity, the level of experimental error is not shown in Figures 3 to 6. The error in the measurements of craze density far from the notch tip was about 10%. For the measurements near the notch tip, the error was about 15 - 20%. The larger value of error was because the high craze density in the close vicinity of the notch tip limits optical microscopy which makes accurate measurements difficult. From these data moments of the distribution with respect to the center of the zone as well as the notch tip were evaluated (Table II). A comparison of the moments shown in Table II shows that the largest difference is ~10% and occurred between the I_{4x} moments with reference to the notch tip. The rest of the differences were always less than 10%. These data and the reproducibility of damage distribution within a process zone in the same material [17] were taken as sufficient indications that damage distributions during crack initiation were reproducible.

Table II: *Inertia Moments for two Configurations of Damage before Crack Initiation.*

Configuration	1	2	1	2
Reference	Notch Tip	Notch Tip	Damage Zone Center	Damage Zone Center
X_c (μm) Y_c	55.0 0.0	52.0 0.0		
I_0 (number)	732	680		
I_{2x} (mm^2)	2.8	2.5	0.65	0.63
I_{2y} (mm^2)	0.46	0.42	0.46	0.42
I_{4x} (mm^4)	0.20×10^{-1}	0.18×10^{-1}	0.11×10^{-2}	0.11×10^{-2}
I_{4y} (mm^4)	0.57×10^{-3}	0.52×10^{-3}	0.57×10^{-3}	0.52×10^{-3}
I_{2x2y} (mm^4)	0.21×10^{-2}	0.18×10^{-2}	0.40×10^{-3}	0.39×10^{-3}

Measurements of damage density within the zones yielded the contours of equal density, ρ, that are shown in Figures 4, 5, and 6, for conditions C1, C2 and C3, respectively. From the experimental data presented in these Figures the center of the damage zone, x_c, can be calculated at each configuration. The data in Figure 7 indicate that the center of gravity of the damage zone increased monotonically with the number of cycles. To investigate the type of transformation the damage density is undergoing during its evolution, the following characteristic scales along the X and Y axes are defined,

$$\frac{I_{2x}}{I_0} = \sigma_x^2, \quad \frac{I_{2y}}{I_0} = \sigma_y^2.$$

Since I_{2x}, I_{2y} are the second moments of the damage zone and I_o is the zeroth moment (which expresses the total amount of crazes within the damage zone) σ_x and σ_y can be looked upon as the measurements of damage spread in the X and Y axes, respectively. Accordingly, for the purpose of comparing damage distributions within the damage zone the following ratios were defined between i_{th} and j_{th} configurations (i= 1, 2, 3 and j=i+1),

$$\frac{\sigma_x^{(j)}}{\sigma_x^{(i)}} = \lambda_{ji}, \quad \frac{\sigma_y^{(j)}}{\sigma_y^{(i)}} = \mu_{ji}, \quad \frac{I_{4x}^{(j)}/I_0^{(j)}}{I_{4x}^{(i)}/I_0^{(i)}} = \Lambda_{ji}^4, \quad \frac{I_{4y}^{(j)}/I_0^{(j)}}{I_{4y}^{(i)}/I_0^{(i)}} = M_{ji}^4, \quad \frac{I_{2x2y}^{(j)}/I_0^{(j)}}{I_{2x2y}^{(i)}/I_0^{(i)}} = H_{ji}^4$$

The type of transformation of damage distribution between consecutive configurations was examined by comparing the following quantities: $(\lambda_{ji}, \Lambda_{ji})$,$(\mu_{ji}, M_{ji})$, and $(\lambda_{ji}\mu_{ji}, H_{ji}^2)$. The above defined ratios for conditions C1, C2, and C3 are shown in Table III. The data in Table III indicate a relatively large difference in the ratios between the first and second configurations for conditions C1.

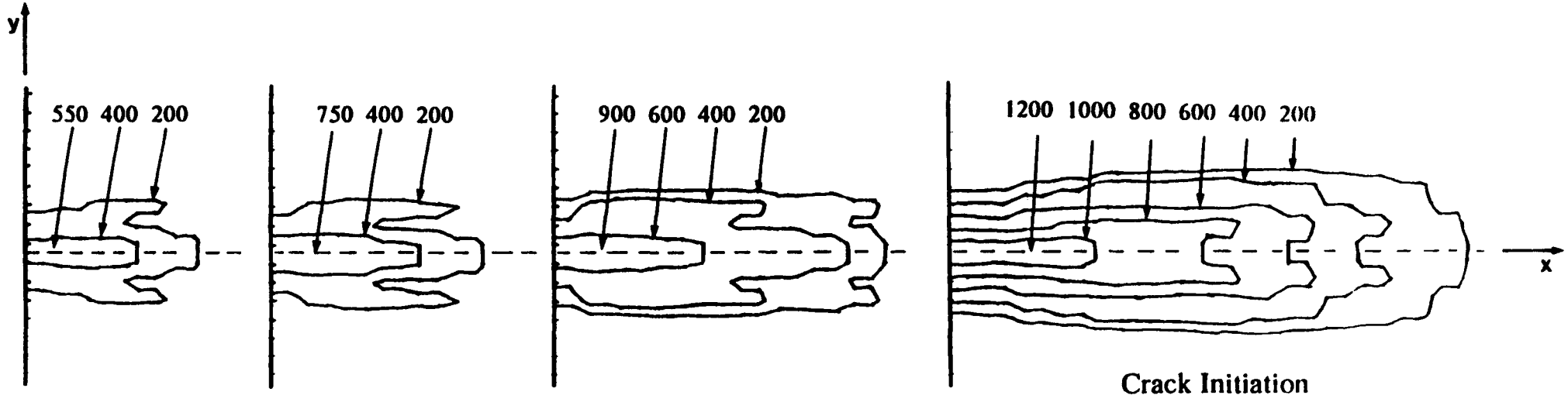

Figure 4 Contours of equal damage density ρ [mm^2/mm^3], at four consecutive configurations before crack initiation (Conditions C1).

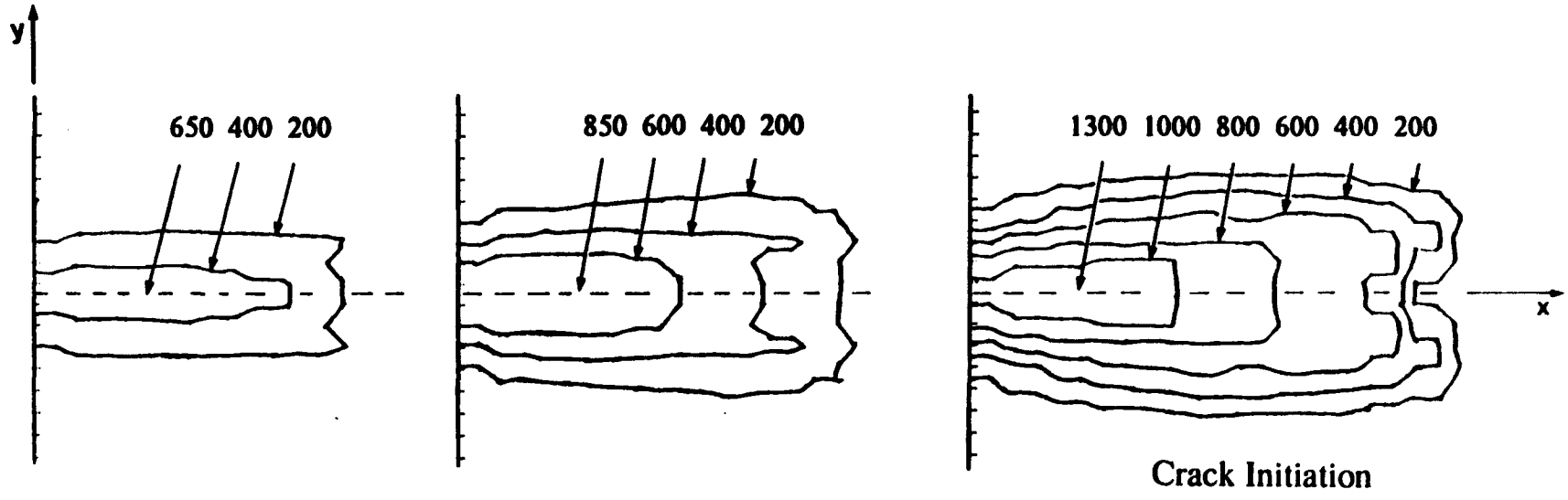

Figure 5 Contours of equal damage density ρ [mm^2/mm^3], at three consecutive configurations before crack initiation (Conditions C2).

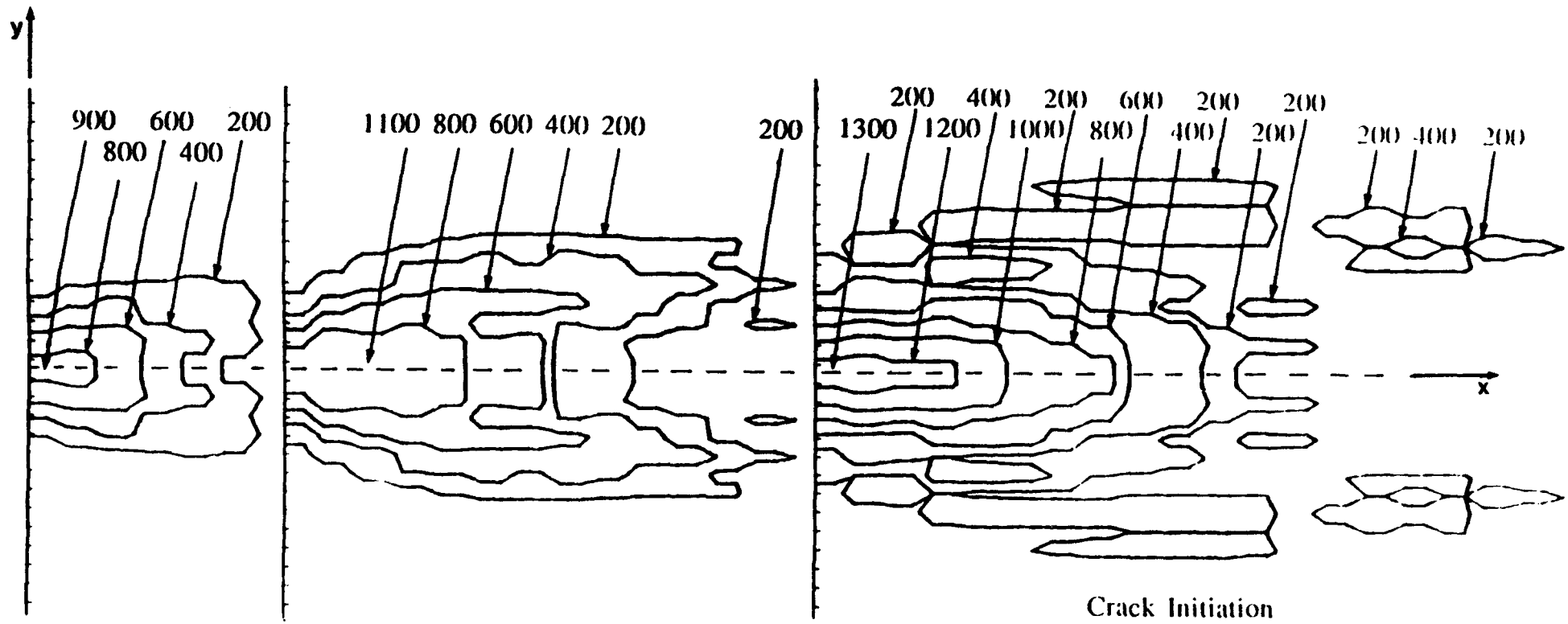

Figure 6 Contours of equal damage density ρ [mm^2/mm^3], at three consecutive configurations before crack initiation (Conditions C3).

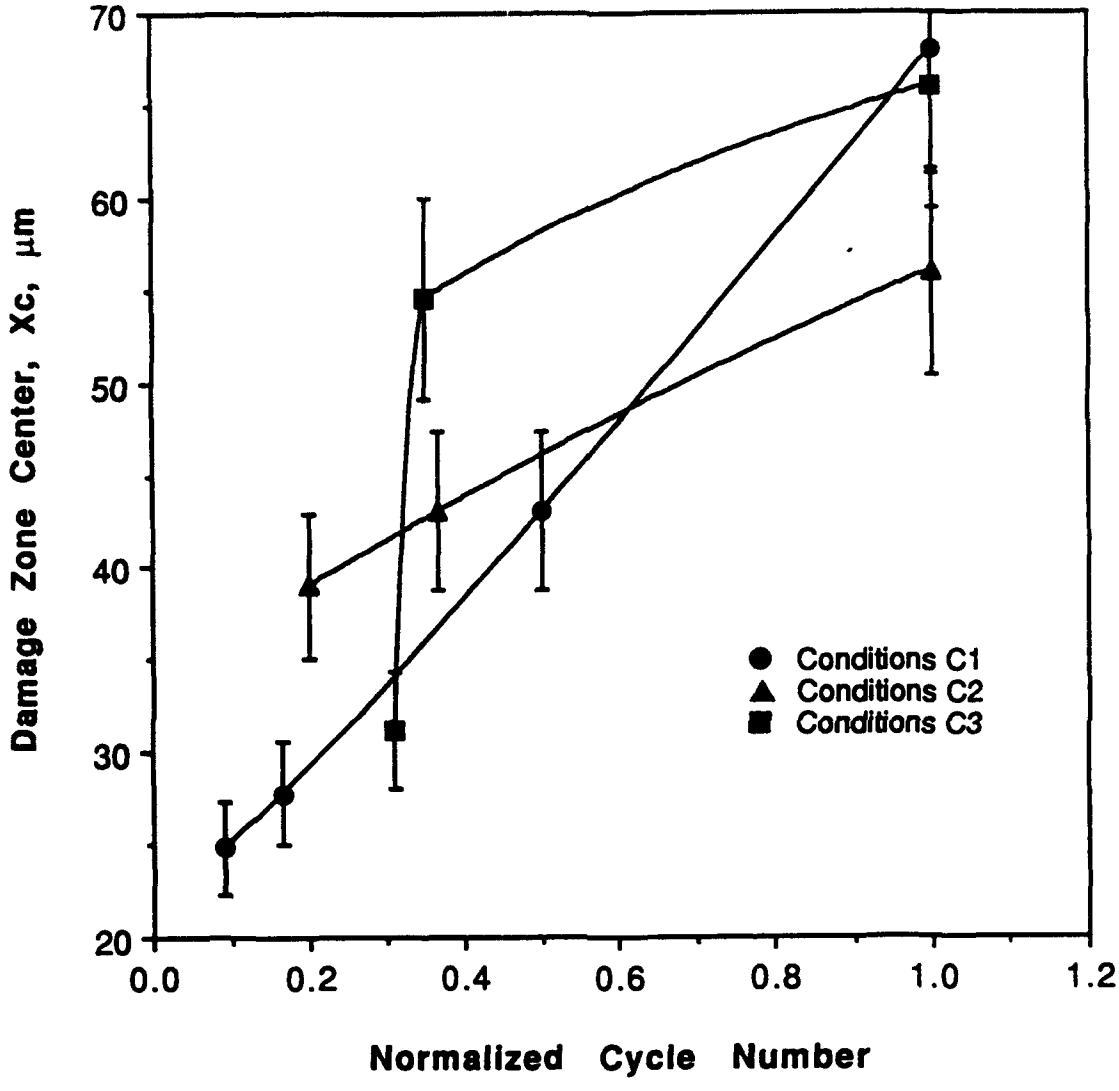

Figure 7 Evolution of the gravity center of the damage zone.

This may be because the system needs some time for damage to be developed so that statistical measurements are meaningful. However, differences between the rest of the ratios were small.

Table III: *Moment Ratio of Damage Distribution at Consecutive Configurations before Crack Initiation.*

Condition C1					
λ_{21}=1.20	Λ_{21}=1.15	μ_{21}=1.02	M_{21}=1.02	$\lambda_{21}\mu_{21}$=1.22	H^2_{21}=1.15
λ_{32}=1.57	Λ_{32}=1.55	μ_{32}=1.30	M_{32}=1.34	$\lambda_{32}\mu_{32}$=2.04	H^2_{23}=2.07
λ_{43}=1.43	Λ_{43}=1.46	μ_{43}=1.30	M_{43}=1.30	$\lambda_{43}\mu_{43}$=1.86	H^2_{23}=1.90
Condition C2					
λ_{21}=1.11	Λ_{21}=1.10	μ_{21}=1.22	M_{21}=1.15	$\lambda_{21}\mu_{21}$=1.35	H^2_{32} = 1.28
λ_{32}=1.17	Λ_{32}=1.17	μ_{32}=1.23	M_{32}=1.23	$\lambda_{32}\mu_{32}$=1.44	H^2_{32}=1.41
Condition C3					
λ_{21}=1.60	Λ_{21}=1.58	μ_{21}=1.38	M_{21}=1.34	$\lambda_{21}\mu_{21}$=2.21	H^2_{21} = 2.10
λ_{32}=1.45	Λ_{32}=1.55	μ_{32}=1.36	M_{32}=1.45	$\lambda_{32}\mu_{32}$=1.97	H^2_{32} = 2.25

The constancy of the ratios λ_{ji}, μ_{ji} between configurations shown in Table III implied that the evolution of damage can be approximated by a linear transformation of the space variables. To obtain the kinematic parameters, the velocity $V_m(\mathbf{x})$ of a point within the zone is expressed by the first two terms of Taylor series around the center of the damage zone,

$$V_m(\mathbf{x}) \approx V_m(0) + V_{m,n}(\mathbf{x})x_n \qquad (1)$$

Here, the first term represents the rigid translation of the damage zone and the second term represents the rotation (anti-symmetric part of $V_{m,n}$) and the deformation (symmetric part of $V_{m,n}$) which in turn can be decomposed into

isotropic expansion and homogeneous distortion of the damage zone. In this section the velocity $V_m(\mathbf{x})$ is expressed in terms of the transformation coefficients λ_{ji} and μ_{ji}. Subsequently the rates of expansion and distortion are evaluated.

The transformation matrix of points with equal damage density between configuration i and j is,

$$D=\begin{bmatrix} \lambda_{ji} & 0 \\ 0 & \mu_{ji} \end{bmatrix} \tag{2}$$

which can be rewritten as,

$$D=\begin{bmatrix} 1+\Delta\lambda_{ji} & 0 \\ 0 & 1+\Delta\mu_{ji} \end{bmatrix} = I+\Delta D \tag{3}$$

where I is the identity matrix and,

$$\Delta D=\begin{bmatrix} \Delta\lambda_{ji} & 0 \\ 0 & \Delta\mu_{ji} \end{bmatrix} \tag{4}$$

Thus, the displacement field within the damage zone can be expressed as,

$$\begin{bmatrix} x+\Delta x \\ y+\Delta y \end{bmatrix}=\begin{bmatrix} 1+\Delta\lambda_{ji} & 0 \\ 0 & 1+\Delta\mu_{ji} \end{bmatrix}\begin{bmatrix} x \\ y \end{bmatrix}+\begin{bmatrix} \Delta x_c \\ 0 \end{bmatrix} \tag{5}$$

where, Δx_c, represents the growth of the center along the x axis. Equation (5) can be rewritten as,

$$\begin{bmatrix} \Delta x \\ \Delta y \end{bmatrix}=\begin{bmatrix} \Delta\lambda_{ji} & 0 \\ 0 & \Delta\mu_{ji} \end{bmatrix}\begin{bmatrix} x \\ y \end{bmatrix}+\begin{bmatrix} \Delta x_c \\ 0 \end{bmatrix} \tag{6}$$

Dividing both sides by the increment of the cycle number ΔN, and setting $\frac{\Delta x}{\Delta N}\rightarrow V_1, \frac{\Delta y}{\Delta N}\rightarrow V_2, \frac{\Delta\lambda_{ji}}{\Delta N}\rightarrow\dot{\lambda}_{ji}, \frac{\Delta\mu_{ji}}{\Delta N}\rightarrow\dot{\mu}_{ji}, \frac{\Delta x_c}{\Delta N}\rightarrow\dot{x}_c$ it is obtained,

$$\begin{bmatrix} V_1 \\ V_2 \end{bmatrix} = \begin{bmatrix} \dot{\lambda}_{ji} & 0 \\ 0 & \dot{\mu}_{ji} \end{bmatrix} \begin{bmatrix} x \\ y \end{bmatrix} + \begin{bmatrix} \dot{x}_c \\ 0 \end{bmatrix} \tag{7}$$

A comparison of Equations (1) and (7) results in,

$$V_m(\mathbf{x}) = \begin{bmatrix} V_1 \\ V_2 \end{bmatrix}, \quad V_m(0) = \begin{bmatrix} \dot{x}_c \\ 0 \end{bmatrix}, \qquad V_{m,n}(\mathbf{x}) = \begin{bmatrix} \dot{\lambda}_{ji} & 0 \\ 0 & \dot{\mu}_{ji} \end{bmatrix} \tag{8}$$

Thus, the rates of expansion $\dot{e}$, and distortion $\dot{d}$, of the damage zone can be expressed as,

$$\dot{e} = \frac{1}{2}(\dot{\lambda}_{ji}+\dot{\mu}_{ji}), \text{ and } \dot{d} = \frac{1}{2}(\dot{\lambda}_{ji}-\dot{\mu}_{ji}) \tag{9}$$

The average values of $\dot{e}$ and $\dot{d}$ as well as the growth of the gravity center of the damage zone for three loading conditions are displayed in Table IV.

Table IV: *Growth Rates of the Gravity Center, Isotropic Expansion and Distortion for three Loading Conditions .*

Configuration	$\Delta X_c/\Delta N$ (x10^4) (μm/cycle)	$\Delta e/\Delta N$ (x10^6), 1/cycle	$\Delta d/\Delta N$ (x10^6), 1/cycle
Conditions C1:			
1-2	1.3	13.0	4.4
2-3	1.5	3.0	1.0
3-4	1.6	2.0	0.7
Conditions C2:			
1-2	4.5	20.0	4.5
2-3	11.8	15.0	3.6
Conditions C3:			
1-2	141.5	27.0	48.0
2-3	4.5	1.75	3.0

The data in Table IV show that while the growth behavior of $\Delta X_c/\Delta N$ depended upon the loading history, the average rates of the damage zone deformation, $\Delta e/\Delta N$ and $\Delta d/\Delta N$, decreased until crack initiation.

It is worth pointing out that damage evolution within a process zone on the same material can be described by a linear transformation [17]. These findings and the results of the present studies indicate that a similar transformation relates damage evolution before crack initiation and during slow crack growth.

The evolution of an average damage density $\langle p \rangle = \Sigma/A$, where Σ is the total number of crazes within the zone and A is the area of the zone with normalized cycle number is shown in Figure 8. (Note that because of the large difference in the cycles to crack initiation between the different experimental conditions, C1: 300,000 cycles, C2: 30,000, C3: 4,000, the number of cycles has been normalized with the respective cycle number at initiation in order to clearly see the trend of $\langle p \rangle$). It is interesting to note that all three sets of data can be approximated by an equation of the form (lines in Figure 8),

$$\langle p \rangle = 1 - \exp(\kappa N) \qquad (10)$$

where N is the number of cycles and κ is a load dependent parameter and equal to $\kappa = 2.5\times10^{-5}$ (C1), 8×10^{-5} (C2), and 1.5×10^{-3} cycle^{-1}(C3). Expression (10) indicates that the dependency of $\langle p \rangle$ on the cycle number is of a damping character. Similar trends of damage accumulation have been reported on smooth specimens of different polymers under creep loads [20].

The data in Figure 8 show that while the rates of damage accumulation were different, craze densities $\langle p \rangle$, at crack initiation were 40,000, 44,200 and 47,000 mm^{-2}, respectively. Note that the error between the extreme values of these densities was 16% while the largest difference from the mean was about 10%.

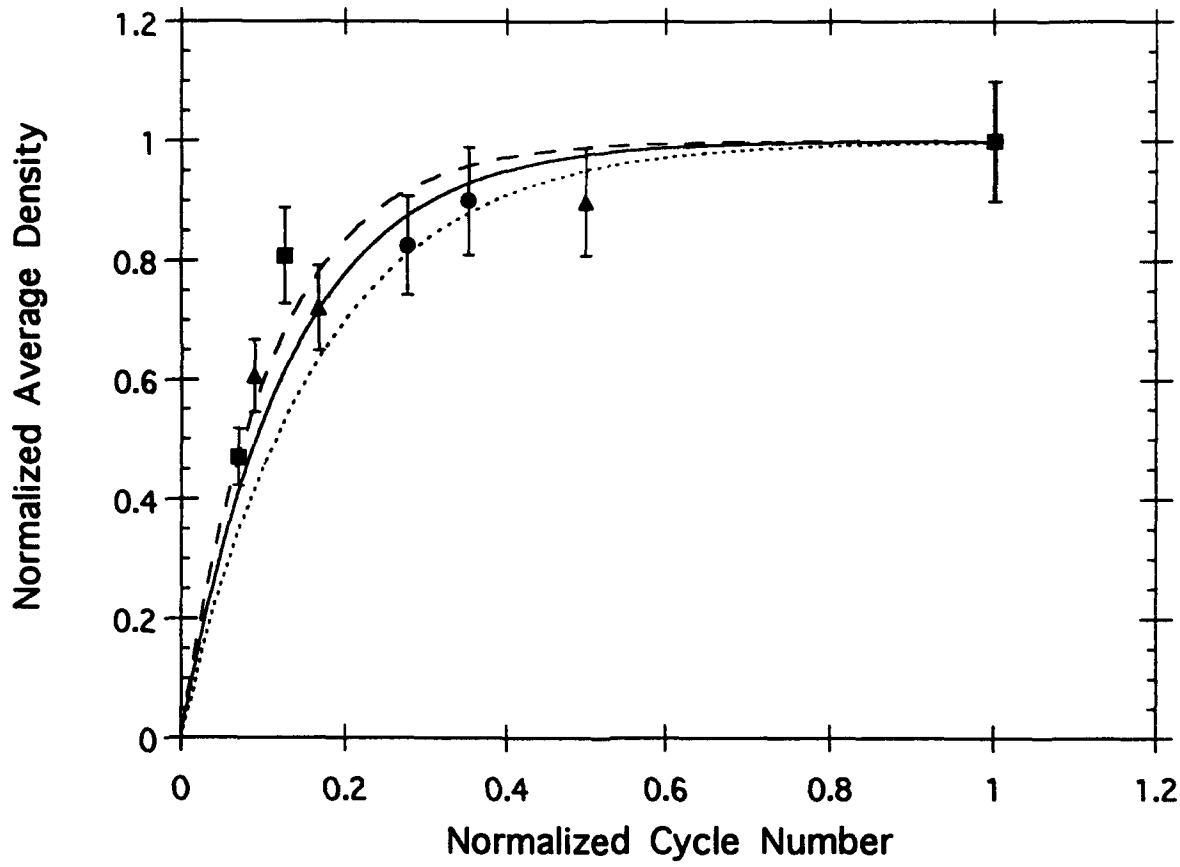

Figure 8 Normalized average density before crack initiation plotted against normalizes cycle number.

Thus one may be led to consider the value of <p> as being independent of the loading conditions at crack initiation. This would be realistic if the density within the zone was constant throughout the zone. However, the results of these studies clearly indicate that damage was not homogeneously distributed (Figures 3 to 6). Thus, an average quantity like <p> may not be indicative of the crack initiation event. On the other hand, crack initiation occurred within a core zone ahead of the notch tip. Morphologies of this highly localized damage zone at initiation for conditions C1 and C3 are shown in Figures 9 and 10, respectively. Within the resolution of the experimental measurements, damage density within the core was about 1,300 mm^2/mm^3 and approximately the same for all loading conditions (Figures 4 to 6). Similar value of damage density has been obtained in the close proximity of the crack tip grown under low frequency fatigue loads [17]. The constancy suggests that a certain level of damage density is required for crack initiation and subsequent crack growth and that this density may be a material parameter. Additional experimental as well as theoretical research is needed to firmly establish this important observation.

The optical micrographs in Figures 9 and 10 bring out an interesting observation. While the density at the notch tip was practically the same, the cycle numbers to crack initiation were drastically different, i. e., 300,000 and 4,000 cycles, respectively. Moreover, damage dissemination around the core zone was quite different (Figures 9 and 10). Thus, one would expect that in the case where large crazes surrounded the core zone would take longer to initiate a crack (Figure 10) due to a greater extent of shielding of the peripheral crazes on the core. However, this was not the case. Therefore, it is assumed that time dependent processes within the damage zone play a more important role than the interaction between the crazes.

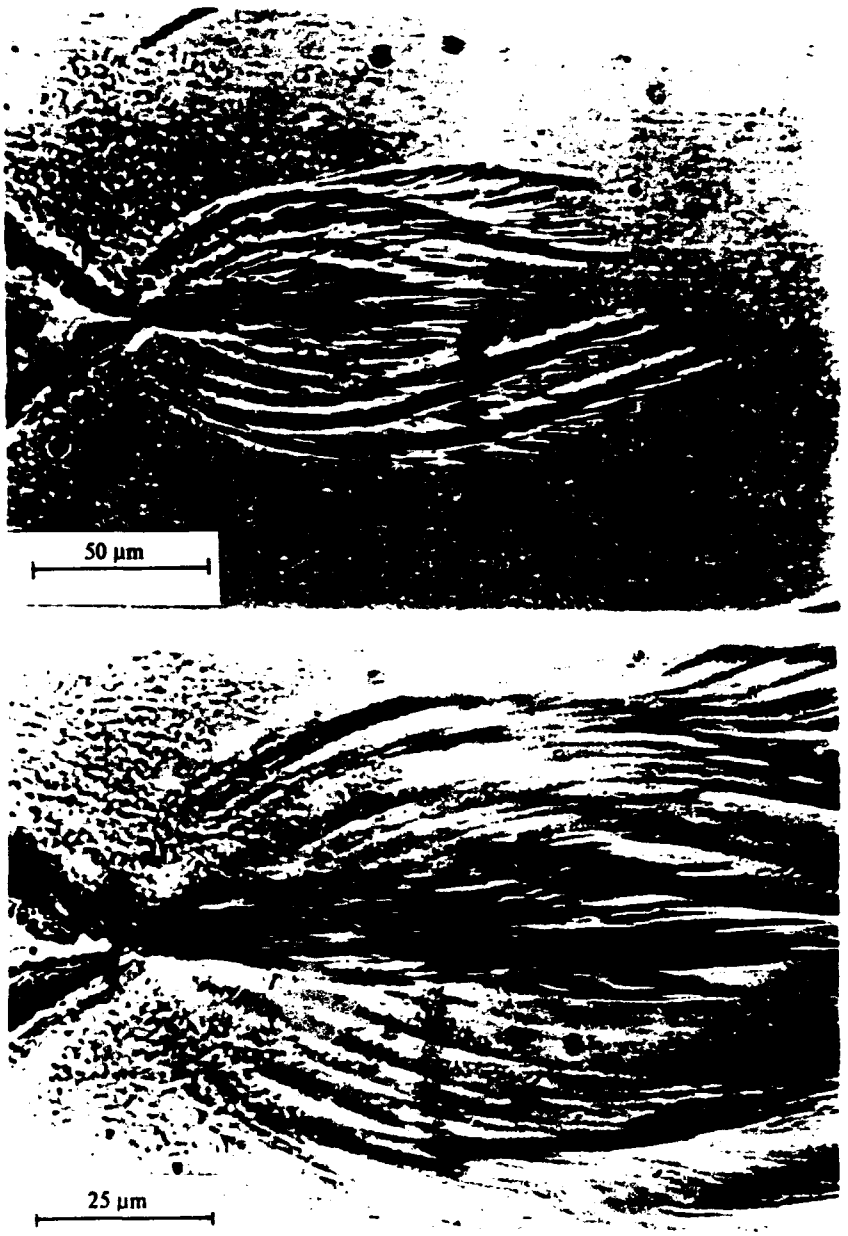

Figure 9 Optical micrographs showing damage distribution at crack initiation (Conditions C1).

Figure 10 Optical micrographs showing damage distribution at crack initiation (Conditions C3).

It was stated earlier that a small crack was observed at the notch tip. This event was associated with crack initiation. An accurate initial crack size, however, was difficult to detect with the use of standard optical observations during the fatigue tests. To evaluate an initial crack size, the specimens were pulled to fracture shortly after crack initiation and the fracture surfaces were observed under an optical microscope. A typical micrograph of the fracture surface morphology near the notch tip is displayed in Figure 11.

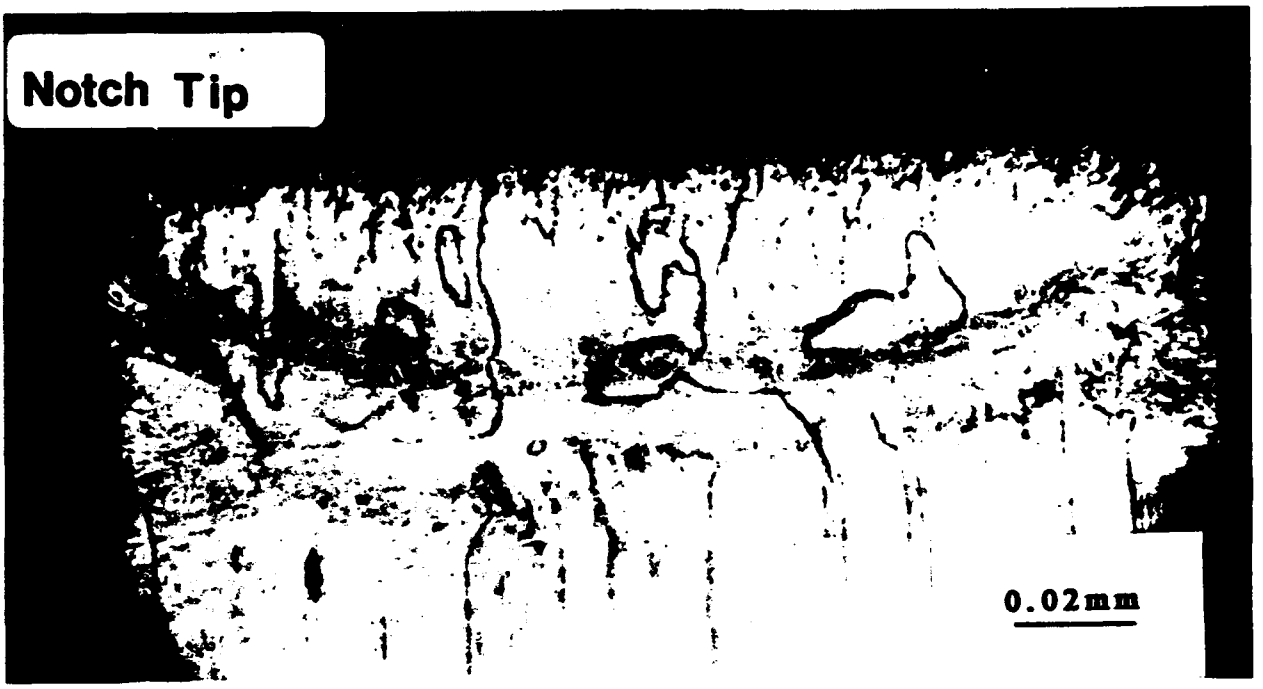

Figure 11 Typical morphology of the fracture surface at crack initiation. Arrows point at the crack front (crack grows from top to bottom).

Note that two distinct morphologies can be seen in the fracture surface: (i) a relatively rough surface from the notch tip which extents up to an arched front, and (ii) the surface with tearing like features. It is assumed that the first morphology is associated with crack initiation. The second morphology corresponds to the crack growth phase resulting from the simple pulling of the specimen after initiation. The morphology shown in Figure 11 suggested that the crack front was not straight. Instead, crack grows more in the middle than at the edges of the specimen surface. The crack length at initiation l_i, taken as the average of five measurements from the notch tip to the curved front is shown in Figure 12 as a function of the stress amplitude. These data indicate that the dependence of the crack length on the applied stress is of the form, $\mathrm{Ln}l_i = B_0 + B_1\sigma$ where B_0 and B_1 are constants.

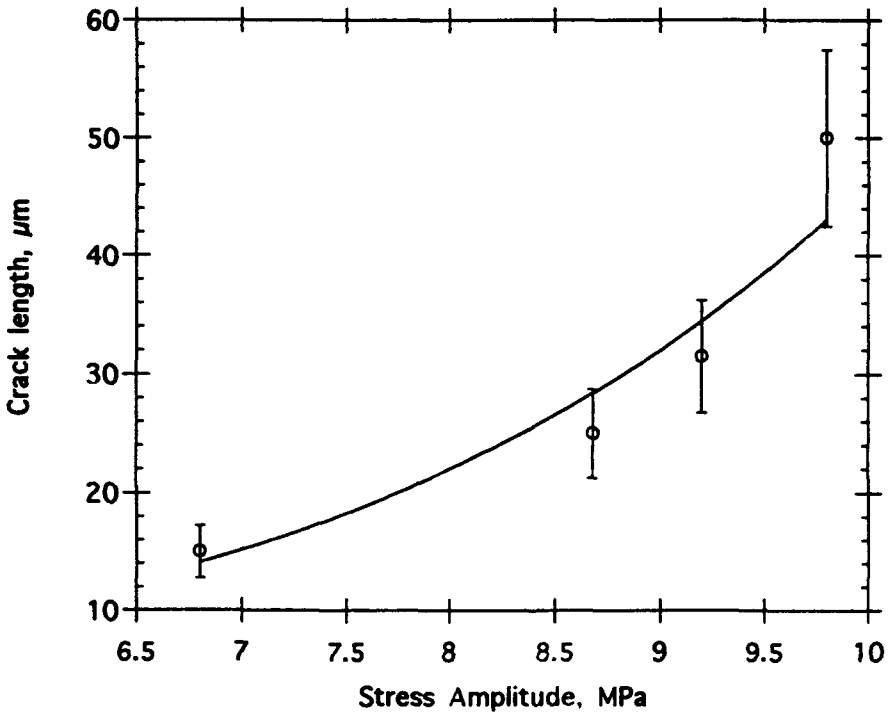

Figure 12 Crack length at crack initiation for various levels of stress amplitude.

Crack initiation times τ_i, plotted against the stress amplitude are shown in Figure 13 (note that $N_i = \nu\tau_i$ where N_i is the number of cycles for crack initiation and ν is the test frequency). These data show that τ_i can be approximated by an expression of the form, $Ln\tau_i = D_0 - D_1\sigma$ where D_0, and D_1 are parameters. Similar relationships have been obtained for different materials including polymers and metals under constant loads and different temperatures [21,22] and have been explained in terms of stress - temperature activated processes at the molecular level. It may be expected that such a relation would not apply in fatigue loads. However, the frequency of the fatigue experiments was very low. Thus, it may be that the material's response is primarily due to the time under load and less due to cycle reversal. Similar results were obtained under cyclic loads in PANB rocket propellant material [23] and other polymeric solids [24].

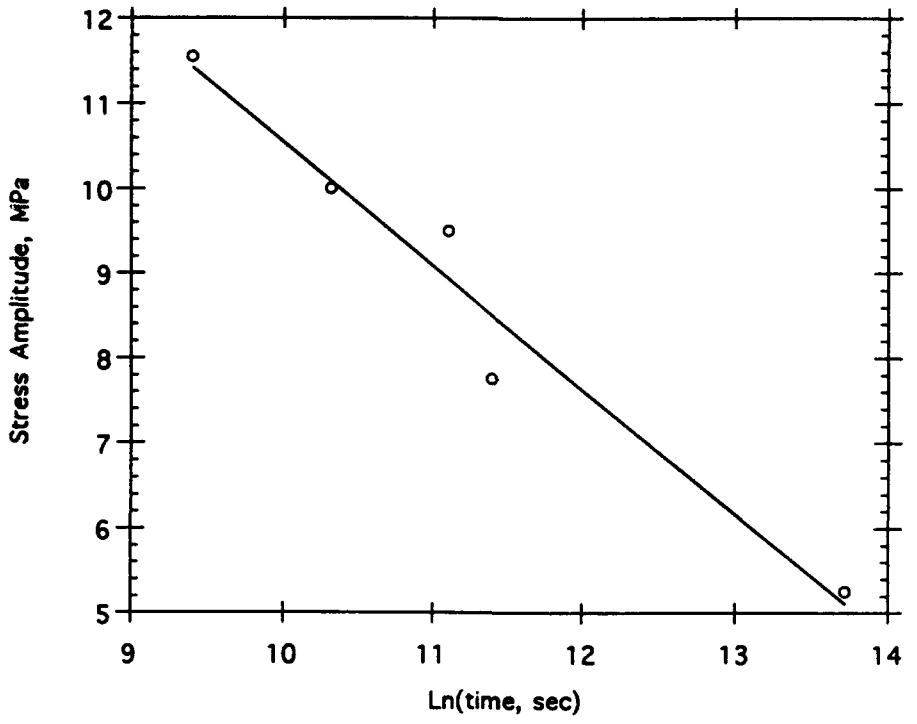

Figure 13 The time to crack initiation plotted against stress amplitude.

4. Concluding Remarks

This investigation was intended to study the phenomenon of crack initiation under low cycle fatigue conditions in an amorphous polymer. The results of the work outlined in this paper have shown that:

1. A damage zone accompanied the process of crack initiation. Within the zone two patterns of damage were distinguished: a core of highly dense damage and a peripheral less dense crazes around the core zone. Crack initiation occurred within the core zone.

2. Damage evolution before crack initiation evolved in a self - similar manner. That is, a linear transformation related the points of equal damage at consecutive configurations of damage.

3. While the growth behavior of the damage zone center depended upon the loading history, the average rates of the damage zone expansion and distortion decreased until crack initiation. Moreover, the dependency of an average damage density with the cycle number exhibited a damping behavior.

4. Damage density within the core of damage was found independent of the loading conditions, however, the pattern of the peripheral crazes was dependent upon the loading conditions. The large difference in crack initiation times was attributed to the role of time dependent processes within the damage zone and the interaction between the crazes.

5. The crack length at initiation was found to increase exponentially with the applied stress.

6. The time to crack initiation was related to the stress level with an exponentially decaying relationship. The results agree with fracture models based on reaction theories.

The results of the present studies and those reported in [17, 18] indicate certain similarities between the characteristics of damage before crack initiation

and during slow crack growth. These are, (a) damage evolution can be described by a linear transformation, (b) the densities of damage within a core zone at crack initiation and during slow crack growth are of the same level.

References

1. J. M. Barsom and S. T. Rolfe, in *Fracture and Fatigue Control in Structures,* 2nd Edition, Prentice Hall, Englewood Cliffs, N. J., (1987).
2. R. W. Hertzberg and J. A. Manson, in *Fatigue in Engineering Plastics,* Academic Press, New York, N. Y. (1980).
3. R. O. Ritchie, *International Metals Reviews,* 5 (1979) 205.
4. C. J. Beevers and R. L. Carlson, in *Fatigue Crack Growth 30 years of Progress',* R. A. Smith ed., Pergamon Press, N.Y. (1986) 89.
5. D. L. Davidson and S. Suresh, eds., in *Fatigue Crack Growth Threshold Concepts,* The Metallurgical Society of AIME , Philadelphia, PA (1984).
6. R. O. Ritchie, in *Advances in Fracture Research, Proc. ICF4',* S. R. Valluri et. al. eds., Pergamon Press, N.Y., 1 (1984) 235.
7. T. C. Lindley and K. J. Nix, in *Fatigue Crack Growth 30 years of Progress,* R. A. Smith ed., Pergamon Press, N.Y. (1986) 53.
8. W. A. Wood, in Treatise *on Materials Science and Technology* Vol. 5, H. Herman, ed., Academic Press, N. Y. (1974) 129.
9. O. Helgeland, *Journal of Institute for Metals* 93 (1965) 570.
10. M. E. Mackay, T. G. Teng and J. M. Schultz, *Journal of Materials Science,,* 14 (1979) 221.
11. N. J. Mills and N. Walker, *Journal of Materials Science,* 15 (1980) 1832.
12. M. Kitagawa, *Journal of Materials Science,* 17 (1982) 2514.
13. J. Botsis, A. Chudnovsky and A. Moet, *International Journal of Fracture,* 33 (1987) 263.
14. M. Kachanov, E. L. E. Montagut, and J. P. Laures, *Mechanics of Materials,* 10 (1990) 59.
15. G. I. Barenblatt and L. R. Botvina, *Soviet Materials Science* (English translation of Fiziko-Khimicheskaya Mechanica Materialov 22 (1986) 52.
16. A. Chudnovsky, *10th U. S. National Conference on Applied Mechanics,* Ed. J. P. Lamb, ASME, Austin, Texas, 1986, p. 97.
17. J. Botsis and X. Q. Zhang, *Journal of Materials Science,* 26 (1991) 1253.
18. J. Botsis, *Journal of Materials Science,* 24 (1989) 2018.
19. G. Margaritis and J. Botsis, *Engineering Fracture Mechanics,* 40 (1991) 1123.
20. V. S. Kuksenko and V. P. Tamuzs, in *Fracture Micromechanics of Polymer Materials,* Martinus Nijhoff, The Hague, (1981).
21. F. Bueche, *Journal of Applied Physics,* 29 (1958) 1231.
22. S. N. Zhurkov, *International Journal of Fracture,* 26 (1984) 295.
23. C. N. Robinson, P. H. Graham, and F. C. Moore, in *Application of Reaction Rate Theory to Solid Propellant Mechanical Behavior,* Vol. 2, Atlantic Res. Corp., Technical Report AFRPL-TR-69-124, (1969).
24. V. R. Regel, and A. M. Leksovsky, *International Journal of Fracture Mechanics,* 3 (1967) 99.